5th SASTech
Iran | Mashhad
May 12 - 17 | 2011
5th Symposium on Advances in Science & Technology

A new 3D Markovian fuzzy approach for increasing the accuracy of measurement of the calcium deposit in 3D CTA images of the coronary artery

Mahdi Mazinani;Rahil Hosseini
Faculty of Electronic engineering, Islamic Azad University,
Shahryar- shahr-e-Qods branch, Tehran, Iran.
mahdi_mazinani@yahoo.com
Paper Reference Number: 0102-678
Name of the Presenter: Mahdi Mazinani

Abstract

Accurate quantification of calcium deposit is an important task in assessing coronary artery disease, especially when the investigation of the disease progress is considered. The reproducibility and robustness of the segmentation algorithm against partial volume effect and noise is critical for an accurate quantification. While there are several approaches for segmentation of the volume of the blood vessel and hard plaque in the literature, the main drawback of these approaches is in making a deterministic decision in terms of assigning a particular voxel to only one type of tissue (such as blood vessel, hard plaque or surrounding area). However in reality, because of the partial volume effect, a voxel may contain more than one tissue type. In particular, using deterministic methods for quantification of the small objects such as thin blood vessels or hard plaque may lead to inaccurate results and higher inter and intra-scan variability.

In this paper, we tackle the problem of the partial volume effect using a 3D adaptive fuzzy algorithm incorporating a Markov random field model. The method is shown to more accurately segment the blood vessel, hard plaque and surrounding tissue areas. The algorithm is applied to several datasets and the outcomes have been judged visually by a qualified radiologist. The proposed algorithm has the potential to be applied for the accurate quantification of the degree of stenosis.

Key words: segmentation, quantification, coronary artery, fuzzy, Markov random field

1. Introduction

Today's digital image processing systems provide powerful tools which can help the radiologist to identify and quantify stenosis. However, there are limitations with image processing techniques in measuring small objects such as calcium deposits in coronary arteries. The partial volume effect (PVE) problem is one of the major issues related to low spatial resolution and motion artifact in digital CTA images. Moreover, the uncertainty arising from the PVE problem leads to inaccurate segmentation and measurement results because a voxel may belong to more than one tissue type but the segmentation method can assigns it to only one type. For tackling these uncertainty problems in image segmentation, several approaches have been described in the literature. These methods can be classified into three main categories: probabilistic methods, fuzzy methods, and a combination of both fuzzy and probabilistic approaches.

Probability theory has been applied more frequently than the other methods. Specifically, Markov random field (MRF) is a probabilistic modeling method which is widely used for incorporating spatial information [8]. As an example, the algorithm presented in [2] utilizes a MRF and stochastic model for the quantification of atherosclerotic plaque in CT images. The approach in [9] segments lung nodule objects by considering spatial properties of objects in the lung, using a combination of Markov Random Field (MRF) and the Expectation–Maximization (EM) algorithm.

Over the last decade, fuzzy sets have been used for managing imprecision in ambiguous circumstances. Several fuzzy methods are proposed in the literature for managing the problem of uncertainty, most commonly the fuzzy c-mean clustering (FCM) algorithm. The main problem with this unsupervised method is the lack of consideration of spatial information, which reduces the accuracy of voxel labeling [3]. Therefore it is required to improve the standard FCM by considering contextual information. For handling this problem, several attempts are reported in the literature to incorporate such spatial information into a fuzzy model [1]. One approach uses smoothing filters before applying fuzzy c-mean clustering, but a consequence is that important information near tissue boundaries will be ignored. Also, the amount of smoothing depends on the noise and artifacts, which cannot be measured automatically. Another approach applies post-processing for smoothing the membership functions of FCM [4]. Multi-scale information in a pyramid style is presented for smoothing the FCM membership value which incorporates spatial constraints into the algorithm [5].

Another effective method which takes advantages of probabilistic and fuzzy approaches incorporates local spatial information directly into the original FCM algorithm’s membership function. In this approach a spatial penalty term is added to membership function to improve the performance of the clustering [1]. An example of this method is the FCM_S algorithm, in which voxels are clustered based on their immediate neighbors. This algorithm calculates the penalty term iteratively and for this reason it is very time consuming [6]. Another example of a combined approach is proposed in [7] which incorporate the prior spatial information based on MRF into the membership function of the standard FCM. However, these methods are not sufficiently robust to noise because they use the FCM algorithm for initial segmentation of the image in order to calculate the conditional probability of the MRF. To address this issue, a novel generalized FCM (NGFCM) algorithm is proposed by Xiaohe et al in [1], which applies MRF spatial constraints into the FCM using a Bayesian approach. This algorithm, which was applied to brain segmentation, improves the robustness of the FCM to noise and artifacts. However, this method is a 2D method and it is not adequate for small digital images such as blood vessels and hard plaque in the coronary arteries which can have high levels of artifact.

In this paper, the original NGFCM algorithm is extend to 3D environment and improved by employing morphological and region growing techniques. The proposed algorithm adaptively tackles the problem of uncertainty in segmentation of the regions in the coronary arteries. The rest of this paper is organized as follows: in section 2, data and material is presented, in section 3 the methodology of research is explained and in section 4, results and analysis are shown. Finally the paper is concluded in section 5.

2.Data and Material

The Data series which are used for evaluation of proposed algorithm are CTA images of coronary arteries from Lausanne Hospital. These 3D images were scanned with the same parameters (120kV, 749 mA, slice thickness 0.6 mm).

3. Methodology of Research

In this section first the basic methodology of NGFCM algorithm which is based on Fuzzy c-mean and Markov random field algorithms will be reviewed. In the next subsection the proposed TDAINGFCM algorithm is explained and discussed step by step in details.

3.1.An overview of NGFCM algorithm

Fuzzy c-means can be applied for clustering an image based on the intensity values of the voxels. The FCM algorithm assigns a membership function to each voxel and defines the degree of belonging of the voxel to the cluster. If X = $\{x_1, x_2, ...x_N\}$ represents the gray-level of an observed image, the standard FCM objective function for clustering is defined as:

$$(U,V) = \sum_{i=1}^{c}\sum_{k=1}^{n} u_{ik}^{m}\ (d_{ik})^2 \tag{1}$$

where $d_{ik} = \|x_k - v_i\|$, V= $\{v_1, ..., v_c\}$ are cluster centers and U=$[u_{ik}]$ is a $c \times n$ matrix and u_{ik} is the ith membership value of the kth input sample x_k. The parameter m determines the amount of fuzziness in the resulting classification and U is the set of membership functions $u_{ik} \in [0,1]$.

The Bayesian framework (MRF) can be used to incorporate spatial information into Eq. 1, which is summarized as follows:

$$p(U) = Z^{-1}\exp\big(W(U)\big) \tag{2}$$

where

$$W(U) = \frac{\beta}{2}\sum_{k=1}^{N} V_{N_k}(U) \tag{3}$$

Z is a normalizing constant, while β is regularization parameter. The potential function of the kth voxel can be computed as follows:

$$V_{N_k}(U) = \sum_{l\in N_k}\sum_{i=1}^{c}(\mu_{ik} - \mu_{il})^2 \tag{4}$$

where N_k is the neighborhood of a given voxel.

By applying the prior and posterior distribution of membership functions and using a logarithmic transformation maximum a posteriori (MAP), estimation of NGFCM is equivalent to minimizing the following objective function [1]:

$$J_m = \sum_{i=1}^{c}\sum_{k=1}^{N}(\mu_{ik})^m(d_{ik})^2 + \frac{\beta}{2}\sum_{i=1}^{c}\sum_{k=1}^{N}\sum_{l\in N_k}(\mu_{ik} - \mu_{il})^2 \tag{5}$$

where $d_{ik} = \|x_k - v_i\|$.

This member function consists of two parts; the first part is the standard FCM function (Eq. 1) and the second part is the penalty term. The parameter β controls the effect of the penalty term and if β=0 then the function reduces to standard FCM. The new membership function has the advantages of FCM and MRF simultaneously. The first part of Eq. 5 is minimized when high membership values are assigned to the voxels with intensities near to the related class and the second term is minimized if the membership values of the adjacent voxels are similar.

3.2.Three dimensional adaptive improved NGFCM algorithm (TDAINGFCM)

In this section, the three dimensional adapted improved NGFCM algorithm (TDAINGFCM) is proposed for the segmentation and quantification of tissues such as hard plaque, blood vessel, and the surrounding areas in the coronary artery. The algorithm describes the step by step procedure as follows:

Step1. Annotation: a Region which includes the stenosis within the coronary artery is manually selected by a radiologist (Fig. 1).

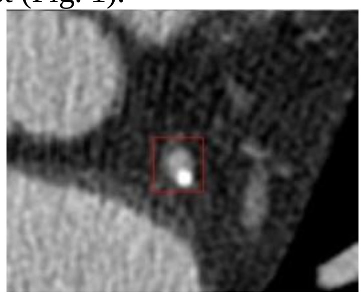

Fig 1: Annotated area on original image for clustering

Step2. Stenosis segmentation: calcium deposit is pre-segmented in 3D by employing a 3D region growing algorithm which starts from the highest intensity in annotated area and segments all connected voxels with the intensity higher than 450 HU as stenosis.

Step3.Volume of interest: the volume of interest (VOF) is selected base on segmented stenosis. A morphological approach (dilation) is applied on segmented stenosis to consider all voxels which may belong to stenosis area. The beginning slice of the volume of interest is selected base on the first slice which contains stenosis and end slice is selected base on the last slice which contains stenosis. By employing a 3D region growing method (with the same seed point in step2), all voxels with intensity more than 200 HU are segmented as the blood vessel and calcium deposit. Then for considering surrounded tissues (in selected slices), a morphological technique (dilation) is applied and the VOF is extracted.

Step4. Apply standard FCM: the standard FCM is applied to the volume of interest to cluster voxels into three regions: blood vessel, calcium deposit and surrounding area. For applying the 2D standard FCM algorithm on VOF, it is applied separately on the 2D images which are achieved from all 2D anatomical direction views (Sagittal, Axial and Coronal) of VOF. In the rest of this paper, each 2D image will be referred as region of interest (ROI). After applying FCM, on each ROI, the centroid of the clusters are checked and if the three centroids are not located in the range of the three considered regions, the number of cluster reduce to two regions and ROI re-clustered. The results of this step are used for choosing the number of region and initializing the NGFCM in the next step to speed up the processing.

Step5. Apply the original NGFCM: The NGFCM is applied to the volume of interest (in the same way which was used in the pervious step) to incorporate the neighborhood information and decrease the influence of the partial volume effect in the standard FCM. Also, the membership function of the NGFCM(μ_{NGFCM}) algorithm is adapted for the segmentation of the coronary arteries.

Step6. Extracting misclassified voxels: Step5 may detect not only the objective regions in each ROI, but also other regions which are not part of the region of interest and have a similar intensity to the ROI. To tackle this problem, a region growing method is applied for recognition of the region of interest (hard plaque) from other regions. The seed is automatically selected by identification of the maximum fuzzy membership value (μ_{Max}) of the particular class (hard plaque). The algorithm selects the largest object and removes the others.

Step7. Region merging: In Step6, the isolated objects are removed; however there is still some mis-segmentation. The reason for this problem is that the intensity (HU) of the surrounding area of the hard plaque decreases gradually (due to the partial volume problem). For this reason, Step5 mis-segments these surrounding voxels as part of a blood vessel. Step 7 applies a morphological operation (an erosion operation followed by a dilation operation) to re-classify voxels labeled blood vessel as hard plaque. At the end of this step, a thresholding method is applied for the segmented regions as follows:

$$\mu_{\text{new}} = \begin{cases} 1 & \mu_{\text{res}} > \tau_1 \\ 0 & \mu_{\text{res}} < \tau_2 \\ \mu_{\text{res}} & \text{else} \end{cases} \tag{6}$$

where μ_{res} is the membership value, and the parameters τ_1, τ_2 are calculated heuristically ($\tau_1, \tau_2 \in [0\ 1]$); in this case $\tau_1 = 0.9$ $\tau_2 = 0.35$ are considered.

Step8.Average membership value: the average membership value for each voxel is calculated base on the three different membership values which is resulted from applying our adapted improved NGFCM algorithm on three anatomical views.

$$\mu_{\text{ave}_{\text{ijk}}} = \frac{\mu_{\text{Sag}_{\text{ijk}}} + \mu_{\text{Axi}_{\text{ijk}}} + \mu_{\text{Cor}_{\text{ijk}}}}{3} \tag{7}$$

Where $\mu_{\text{ave}_{\text{ijk}}}$is average membership value for voxel V(i,j,k) and $\mu_{\text{Sag}_{\text{ijk}}}$, $\mu_{\text{Axi}_{\text{ijk}}}$, $\mu_{\text{Cor}_{\text{ijk}}}$ are membership values of that voxel in Sagittal, Axial and Coronal views respectively.

Step9. Hard plaque quantification: For measuring the volume of calcium deposit the result of step 8 is used as follows:

$$\text{Vol}_{\text{cal}} = \sum_{\text{ijk}\epsilon\text{VOF}} \mu_{\text{ave}_{\text{ijk}}} * \text{V}l \tag{8}$$

where Vol_{cal} is the quantified value for hard plaque, ijk are coordinate of the of voxels in the Volume of interest, $\mu_{\text{new}_{\text{ik}}}$ is the membership value which is calculated in step 8 and $\text{V}l$ is the volume of each voxel.

4. Results and Analysis

In order to verify the robustness of the proposed TDAINGFCM algorithm, we compared it's performance against three standard methods: a deterministic k-means clustering approach, and the standard FCM and NGFCM algorithms. The algorithms are applied to CTA images of coronary arteries, including 10 CTA images from Lausanne hospital with the same parameters (120kV, 749 mA, slice thickness 0.6 mm). The results have been approved visually by a qualified radiologist. The segmentation objective is to cluster the image into three areas, i.e. hard plaque, blood vessel and surrounding area with average HUs of 1000, 300, and 50 respectively.

Fig s. 2~3 illustrate the results of applying the methods to the same small image region in axial view. Fig. 2(a) is an example region of interest which was selected by a radiologist.

Fig. 2(b) shows the corresponding HU values. The result of k-means clustering is shown in Fig. 2(c). Fig. 2(e) shows the result of applying the standard FCM algorithm, with the corresponding degree-of-membership table shown in Fig. 2(f). Comparing the results of

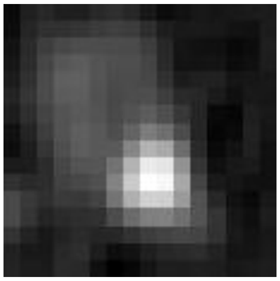

(a)

-81	41	86	45	35	91	124	84	-4	-63	-33	0	-11	-2	15	19
-62	-69	138	136	157	199	220	106	26	29	2	8	0	-31	-40	20
-27	100	208	268	291	290	286	283	212	79	-16	-38	-46	-86	-70	30
-8	115	255	356	375	333	304	296	247	100	-25	-31	-20	-67	-47	27
28	137	283	392	396	334	288	288	265	136	23	42	47	-20	-11	-3
66	163	281	375	380	323	268	290	306	207	105	83	15	-48	6	-7
31	127	241	331	364	331	275	324	384	301	180	75	-77	-94	35	2
-42	73	212	324	390	359	306	416	554	483	285	71	-100	-73	51	-12
-59	31	159	302	384	358	373	611	859	805	470	98	-78	-31	41	-38
14	28	109	259	333	345	504	858	1177	1140	684	157	-44	-2	13	-48
143	98	117	231	263	312	590	993	1281	1250	803	244	7	-13	-43	-38
268	182	134	185	182	240	516	837	1024	1012	723	321	80	-38	-77	-2
272	158	71	101	118	139	286	467	571	584	489	330	156	-5	-52	25
153	60	6	61	102	77	79	145	213	245	259	240	142	12	-31	6
53	3	-2	85	121	31	-53	-32	42	81	104	116	60	-17	-20	8
64	22	17	97	89	-47	-135	-91	-14	29	34	41	32	-4	16	26

(b)

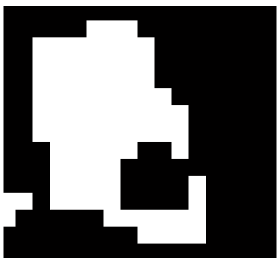

(c)

0	0	0	0	0	0	0	0	0	0	0	0	0	0	0	0
0	0	0	0	0	1	1	1	0	0	0	0	0	0	0	0
0	0	1	1	1	1	1	1	1	0	0	0	0	0	0	0
0	0	1	1	1	1	1	1	1	0	0	0	0	0	0	0
0	0	1	1	1	1	1	1	1	0	0	0	0	0	0	0
0	0	1	1	1	1	1	1	1	1	0	0	0	0	0	0
0	0	1	1	1	1	1	1	1	1	1	0	0	0	0	0
0	0	1	1	1	1	1	1	1	1	1	0	0	0	0	0
0	0	0	1	1	1	1	1	0	0	1	0	0	0	0	0
0	0	0	1	1	1	1	0	0	0	0	0	0	0	0	0
0	0	0	1	1	1	1	0	0	0	0	1	0	0	0	0
1	1	0	1	1	1	1	0	0	0	0	1	0	0	0	0
1	0	0	0	0	0	1	1	1	1	1	1	0	0	0	0
0	0	0	0	0	0	0	0	1	1	1	1	0	0	0	0
0	0	0	0	0	0	0	0	0	0	0	0	0	0	0	0

(d)

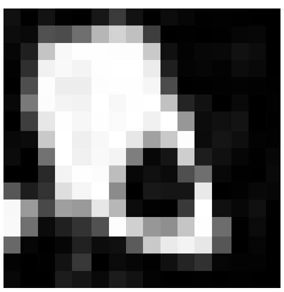

(e)

0.01	0.01	0	0.06	0.01	0.01	0.07	0	0.01	0.01	0.01	0.01	0.01	0.01	0.01	0.01
0.01	0	0.11	0.11	0.21	0.5	0.66	0.56	0.07	0.01	0.01	0.01	0.01	0.01	0.01	0.01
0.01	0.02	0.57	0.92	0.97	0.97	0.97	0.96	0.6	0	0.01	0.01	0.01	0.01	0.01	0.01
0.01	0.04	0.87	0.99	0.97	0.99	0.99	0.98	0.83	0.02	0.01	0.01	0.01	0.01	0.01	0.01
0.01	0.11	0.96	0.95	0.94	0.99	0.97	0.97	0.91	0.11	0.01	0.01	0.01	0.01	0.01	0.01
0	0.24	0.95	0.96	0.99	0.92	0.97	0.99	0.56	0.02	0	0.01	0.01	0.01	0.01	0.01
0.01	0.07	0.8	0.99	0.98	0.99	0.94	0.99	0.96	0.99	0.36	0	0.01	0.01	0.01	0.01
0.01	0	0.6	0.99	0.95	0.98	0.99	0.91	0.65	0.8	0.96	0	0.01	0.01	0.01	0.01
0.01	0.01	0.22	0.99	0.96	0.98	0.97	0.52	0.04	0.1	0.82	0.01	0.01	0.01	0.01	0.01
0.01	0.01	0.03	0.88	0.99	0.99	0.76	0.04	0.06	0.04	0.34	0.21	0.01	0.01	0.01	0.01
0.14	0.01	0.05	0.73	0.89	0.99	0.56	0	0.09	0.08	0.1	0.81	0.01	0.01	0.01	0.01
0.92	0.37	0.1	0.39	0.37	0.8	0.73	0.06	0.01	0	0.25	0.99	0	0.01	0.01	0.01
0.93	0.21	0	0.02	0.05	0.12	0.97	0.83	0.61	0.58	0.79	0.99	0.2	0.01	0.01	0.01
0.18	0	0.01	0	0.02	0	0	0.14	0.61	0.82	0.88	0.79	0.13	0.01	0.01	0.01
0	0.01	0.01	0	0.06	0.01	0.01	0.01	0.01	0	0.02	0.04	0	0.01	0.01	0.01
0	0.01	0.01	0.01	0.01	0.01	0.01	0.01	0.01	0.01	0.01	0.01	0.01	0.01	0.01	0.01

(f)

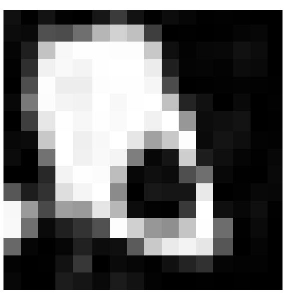

(g)

0.1	0.07	0.14	0.09	0.1	0.21	0.32	0.18	0.07	0.07	0.05	0.04	0.04	0.04	0.04	0.07
0.07	0.08	0.31	0.35	0.47	0.67	0.75	0.67	0.28	0.04	0.01	0.01	0.01	0.03	0.03	0.05
0.06	0.18	0.67	0.90	0.94	0.96	0.96	0.93	0.69	0.12	0.02	0.03	0.03	0.06	0.05	0.05
0.06	0.26	0.86	0.96	0.95	0.99	0.99	0.98	0.84	0.2	0.03	0.02	0.02	0.05	0.04	0.05
0.08	0.36	0.92	0.93	0.93	0.99	0.99	0.98	0.91	0.36	0.04	0.02	0.02	0.02	0.01	0.04
0.12	0.47	0.92	0.95	0.95	0.99	0.97	0.99	0.97	0.71	0.21	0.09	0.01	0.03	0.01	0.04
0.07	0.30	0.83	0.98	0.97	0.99	0.98	0.98	0.93	0.93	0.55	0.11	0.06	0.07	0.01	0.04
0.07	0.12	0.72	0.97	0.94	0.97	0.98	0.88	0.64	0.77	0.86	0.12	0.08	0.05	0.02	0.04
0.07	0.05	0.46	0.95	0.95	0.97	0.93	0.5	0.06	0.11	0.76	0.2	0.07	0.03	0.01	0.05
0.06	0.05	0.25	0.88	0.98	0.97	0.73	0.06	0.06	0.05	0.32	0.42	0.06	0.01	0.01	0.06
0.36	0.18	0.28	0.78	0.92	0.96	0.55	0.02	0.09	0.08	0.11	0.75	0.06	0.02	0.03	0.06
0.83	0.54	0.32	0.56	0.6	0.83	0.7	0.08	0.02	0.02	0.25	0.89	0.16	0.04	0.06	0.04
0.83	0.42	0.11	0.17	0.25	0.37	0.86	0.77	0.58	0.56	0.76	0.91	0.42	0.03	0.04	0.05
0.39	0.08	0.03	0.05	0.14	0.11	0.14	0.38	0.68	0.8	0.84	0.77	0.33	0.03	0.02	0.04
0.08	0.02	0.02	0.08	0.18	0.03	0.05	0.05	0.07	0.15	0.21	0.23	0.07	0.02	0.02	0.04
0.11	0.05	0.05	0.15	0.13	0.07	0.12	0.09	0.05	0.06	0.06	0.07	0.06	0.04	0.04	0.07

(h)

Fig.2: (a) The original image, (b) HU table for original image. (c) K-Mean clustering result, (d) table of K-means clustering result, (e) FCM clustering result, (f)table of FCM clustering result, (g) NGFCM clustering result, (h) table of NGFCM clustering result.

these two methods, there are some voxels in Fig. 2(d) for which the HU value is further from the average HU for blood vessel and hence may belong to more than one region. This fact is not accounted for in deterministic clustering (Fig. 2(b)), although, the standard FCM gives some consideration to the degree-of-membership of a voxel to more than one region. The drawback of the standard FCM is that spatial information of the voxels is not considered during the clustering method and some voxels are misclassified, as are shown in Fig. 2(f).

For the NGFCM algorithm, by incorporating spatial information using MRKV approach an improved result is achieved over the standard FCM algorithm. The algorithm considers the neighborhood information of one voxel. In the implementation of this algorithm an 8 neighborhood scheme is considered for N_k, and the parameter m is set to 2. Selection of β is very important and has influence on the labelling performance. In this paper, the cross-validation method is used for selecting β [5]. For our application, β is considered in [0, 1] and was fixed at β=7e-4. The result of applying this algorithm is shown in Fig. 2(g). Because of the uncertainty associated with the partial volume effect and noisy images, the NGFCM method is inadequate for labeling small regions with high levels of artifact. As shown in Fig. 2(h), after applying the NGFCM algorithm there are still some voxels which have been clustered incorrectly. To address this problem, the proposed TDAINGFCM algorithm is applied for labeling the coronary artery images. As is demonstrated in Figs. 3(a) ~3(b), step 6 removes the disconnected regions with similar intensity and step 7 removes all the voxels which do not belong to the ROI and assigns them to the hard plaque. Figs. 3(c) ~3(d) illustrate the results of step 7 and the corresponding membership values respectively. In step 8 the average membership value is calculated base on 3 membership values which are calculated from three different anatomical views and finally in

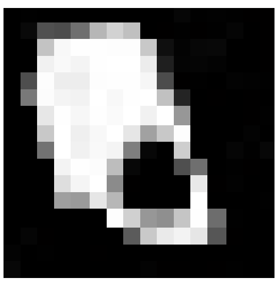

(a)

0	0	0	0	0	0	0	0	0	0	0	0	0	0	0	0
0	0	0.31	0.35	0.47	0.67	0.75	0.67	0	0	0	0	0	0	0	0
0	0	0.67	0.90	0.94	0.96	0.96	0.93	0.69	0	0	0	0	0	0	0
0	0	0.86	0.96	0.95	0.99	0.99	0.98	0.84	0	0	0	0	0	0	0
0	0.36	0.92	0.93	0.93	0.99	0.99	0.98	0.91	0.36	0	0	0	0	0	0
0	0.47	0.92	0.95	0.95	0.99	0.97	0.99	0.97	0.71	0	0	0	0	0	0
0	0	0.83	0.98	0.97	0.99	0.98	0.98	0.93	0.93	0.55	0	0	0	0	0
0	0	0.72	0.97	0.94	0.97	0.98	0.88	0.91	0.77	0.86	0	0	0	0	0
0	0	0.46	0.95	0.95	0.97	0.93	0.5	0	0	0.76	0	0	0	0	0
0	0	0	0.88	0.98	0.97	0.73	0	0	0	0.32	0.42	0	0	0	0
0	0	0	0.78	0.92	0.96	0.55	0	0	0	0	0.75	0	0	0	0
0	0	0	0.56	0.6	0.83	0.7	0	0	0	0	0.89	0	0	0	0
0	0	0	0	0	0.37	0.86	0.77	0.58	0.56	0.76	0.91	0	0	0	0
0	0	0	0	0	0	0	0.38	0.68	0.8	0.84	0.77	0	0	0	0
0	0	0	0	0	0	0	0	0	0	0	0	0	0	0	0
0	0	0	0	0	0	0	0	0	0	0	0	0	0	0	0

(b)

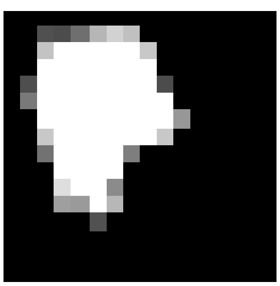

(c)

0	0	0	0	0	0	0	0	0	0	0	0	0	0	0	0
0	0	0.31	0.35	0.47	0.67	0.75	0.67	0	0	0	0	0	0	0	0
0	0	0.67	1	1	1	1	1	0.69	0	0	0	0	0	0	0
0	0	0.86	1	1	1	1	1	1	0	0	0	0	0	0	0
0	0.36	1	1	1	1	1	1	1	0.36	0	0	0	0	0	0
0	0.47	1	1	1	1	1	1	1	1	0	0	0	0	0	0
0	0	0.83	1	1	1	1	1	1	1	0.55	0	0	0	0	0
0	0	0.72	1	1	1	1	1	1	0.77	0.86	0	0	0	0	0
0	0	0.46	1	1	1	1	0.5	0	0	0	0	0	0	0	0
0	0	0	1	1	1	1	0	0	0	0	0	0	0	0	0
0	0	0	0.78	1	1	0.55	0	0	0	0	0	0	0	0	0
0	0	0	0.56	0.6	0.83	0.7	0	0	0	0	0	0	0	0	0
0	0	0	0	0	0.37	0	0	0	0	0	0	0	0	0	0
0	0	0	0	0	0	0	0	0	0	0	0	0	0	0	0
0	0	0	0	0	0	0	0	0	0	0	0	0	0	0	0
0	0	0	0	0	0	0	0	0	0	0	0	0	0	0	0

(d)

Fig 3: (a) NGFCM clustering result after extracting misclassified voxels, (b) The corresponding table of (a), (c) TDAINGFCM clustering result in a slice, (d) table of TDAINGFCM clustering result in a slice.

5. Conclusions

In this paper a three dimensional improved and adaptive algorithm based on the FCM and MRF model is proposed and applied for tackling the partial volume effect problem in segmentation and quantification of volume of the hard plaque in 3D CTA images of the coronary arteries.

The proposed algorithm has implemented and the results reveal the superior performance of the algorithm compared to the FCM and NGFCM algorithms for accurate segmentation of the small regions in the coronary arteries. Our future work is to measure the heuristic parameters of the algorithm by employing optimization techniques on an image phantom and applying the results of this algorithm to a quantification of the degree of stenosis.

Acknowledgements
I would like to say thank you to all the experts and specialists in the Lausanne hospital especially Dr. Qandli who were helped me for preparing the CTA images and assessment of the results.

References

[1] Xiaohe Li, Taiyi ZHANG, and Zhan QU (2008). Image Segmentation Using Fuzzy Clustering with Spatial Constraints Based on Markov Random Field via Bayesian Theory. *IEICE TRANS. FUNDAMENTALS.* E91–A (3), 723-729.

[2] Jamshid Dehmeshki, Xujiong Ye, Hamdan Amin, Maryam Abaei, XinYu Lin, and Salah D. Qandli (2007).Volumetric Quantification of Atherosclerotic Plaque in CT Considering Partial Volume Effect. *IEEE Trans. on Medical Imaging*. 26(3), 273-282.

[3] S.C. Chen and D.Q. Zhang (2004). Robust image segmentation using FCM with spatial constraints based on new kernel-induced distance measure. *IEEE Trans. Syst. Man Cybern. B.* 34(4) , 1907–1916.

[4] Y.A. Tolias and S.M. Panas (1998). On applying spatial constraints in fuzzy image clustering using a fuzzy rule-based system. *IEEE Signal Process.* 5(10), 245–247.

[5] D. L. Pham (2001). Spatial models for fuzzy clustering. *Computer Vision and Image Understanding.* 84(2), 285–297.

[6] M.N. Ahmed, S.M. Yamany, N. Mohamed, A.A. Farag, and T. Moriarty (2002). A modified fuzzy c-means algorithm for bias field estimation and segmentation of MRI data. *IEEE Trans. Med. Imaging*. 21(3), 193–199.

[7] Y.Q. Feng and W.F. Chen (2004). Brain MR Image segmentation using fuzzy clustering with spatial constraints based on Markov random field theory. *Lect. Notes Com. Sci.*31(50),188–195.

[8] S. Z. Li (1995). *Markov Random Field Modeling in Computer Vision.* Verlag, Springer.